Results Comparison for Hat-shaped, Double-notch and Punch Testing of Split Hopkinson Shear Bar Technique

Bagus Budiwantoro, Iffah Faizah, Dini A. Prabowo, Burhan Febrinawarta & Muhammad A. Kariem*

Faculty of Mechanical and Aerospace Engineering, Institut Teknologi Bandung, Jalan Ganesha No. 10, Bandung 40132, Indonesia
*E-mail: kariem@edc.ms.itb.ac.id

Abstract. The split Hopkinson shear bar (SHSB) test is a modification of the high rate-impact test using a split Hopkinson pressure bar (SHPB). The SHSB has been developed for a variety of techniques, for example, the hat-shaped (circular or flat), double-notch, and punch (with or without notch) techniques. The main purpose of this study was to compare these three techniques to determine the shear stress-shear strain of aluminum alloy 2024-T351. The study was conducted using the Abaqus/CAE® software. The circular hat-shaped and punch (with and without notch) techniques used a quarter-section solid 3D model. The flat hat-shaped and double-notch techniques used a half-section solid 3D model. This study successfully tested and compared the three SHSB techniques, with a number of considerations, i.e. the same parameter values for kinetic energy, shear area and shear angle. Each technique has its own advantages and disadvantages in terms of force equilibrium, flow stress fluctuation, constant strain rate, machine-ability, ease of experiment, etc. The optimum technique among the three is the hat-shaped technique.

Keywords: *double-notch; hat-shaped; Hopkinson bar; punch; SHSB.*

1 Introduction

The split Hopkinson pressure bar (SHPB) is a testing device that is used to generate the stress-strain curve of materials at high strain rates from 10^2 to 10^4 s^{-1} [1]. The technique was named after Hopkinson's family [2-4] for their contribution to the pioneering of high-strain testing. It was developed further by Davies [5], who used a parallel plate condenser for measuring the axial and radial displacements of the free end of the bar. Kolsky [6] used two pressure bars instead of one, with a specimen, such as polythene, natural and synthetic rubbers, polymethylmethacrylate (PMMA), copper or lead, sandwiched in between.

Since then, several major developments of the SHPB technique have been done. One of the modifications of the SHPB technique is the split Hopkinson shear bar (SHSB), which uses the same principles as the SHPB but a different load

Received August 19th, 2019, 1st Revision October 9th, 2019, 2nd Revision October 17th, 2019, Accepted for publication November 4th, 2019.
 ISSN: 2337-5779, DOI: 10.5614/j.eng.technol.sci.2019.51.6.5

type, i.e. a shearing load. Shear deformation is a major deformation mode that occurs in engineering applications, such as punching, grinding, machining, and forming. In general, three types of shear testing methods have been developed, i.e. the shear test with hat-shaped test [7-10], the punch test [11] and the double-notch shear test [12-14]. Each has a different specimen geometry, shear area, shear angle and pressure bar geometry. Figure 1 shows a schematic of these three techniques, while Figure 2 shows the specimen geometry and shear area.

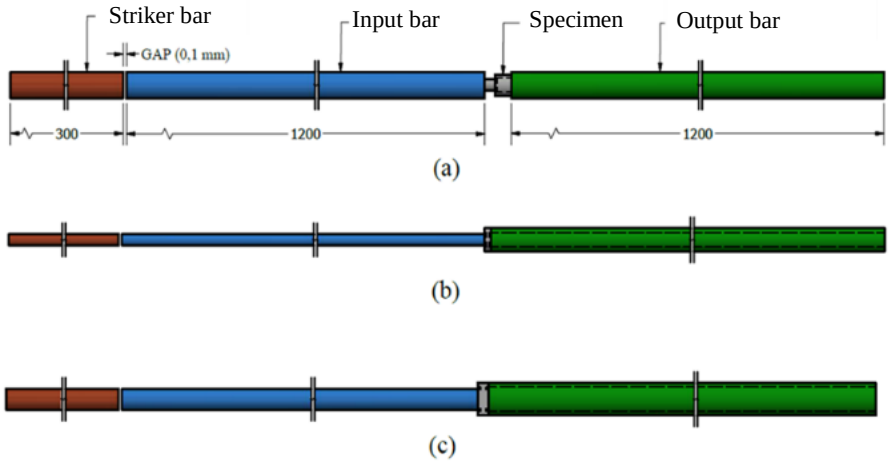

Figure 1 Schematic of SHSB testing apparatus: (a) hat-shaped, (b) punch, and (c) double-notch. All units in mm.

Testing on bulk material can be conducted using a circular hat-shaped (Figure 2(a)) or a flat hat-shaped specimen (Figure 2(b)). This will generate a more concentrated shear stress on a narrow area. For material that cannot normally experience localized shearing, the geometry of a hat-shaped specimen generates shear stress until failure. Another benefit of using a hat-shaped specimen is the simplicity of determining the specimen deformation, which is needed for further data processing. However, when it comes to the post-mortem observation of the specimen, a difficulty appears as there will be a sub-surface surrounding the shear band, which makes it impossible to measure the temperature and local strain [8].

Another test for bulk material is the double-notch test (Figure 2(c)). The specimen will likely receive shear stress during the test. A double-notched specimen creates a very short gauge length, which will increase the maximum strain rate that can be achieved. By using this specimen, a non-uniform stress distribution will not be achieved in the first state of yielding and also it will not create a pure shear state after the strain exceeds 20% [15]. To overcome the non-uniform stress distribution, a set of clamping devices is commonly used,

but this will generate another reflected wave so that the transmitted wave cannot be processed further. Campbell and Ferguson have conducted a test on double-notched mild steel that reached strain rates of up to 40,000 s^{-1} [13].

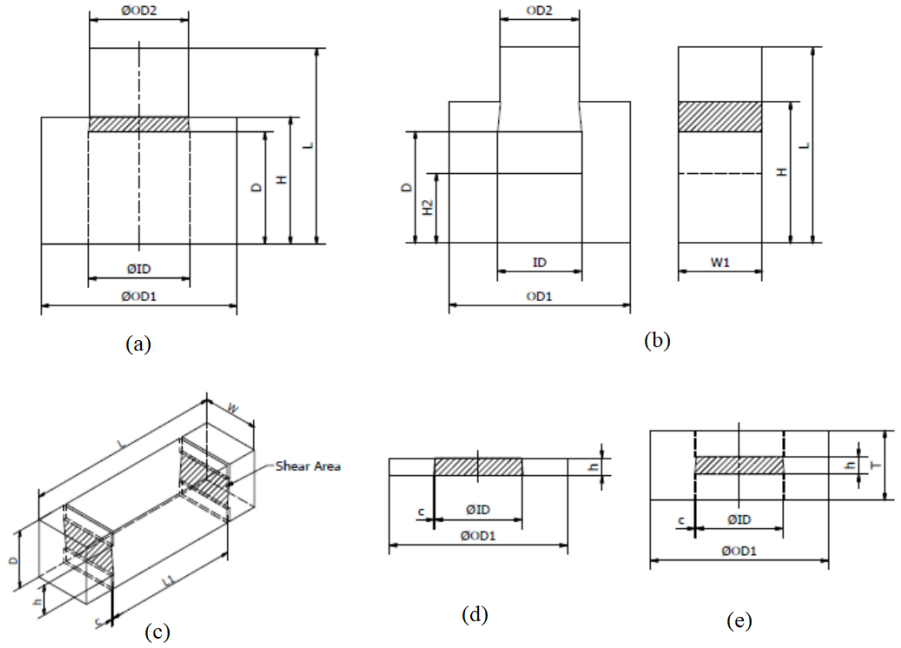

Figure 2 Geometry of specimens: (a) circular hat-shaped (C-HS), (b) flat hat-shaped (F-HS), (c) double-notch (D-N), (d) punch without notch (P-nN), and (e) punch with notch (P-N).

In the testing of sheet metal, the punch test (Figure 2(d)) is commonly used. This test uses a solid input bar and a hollow output bar, where its inner diameter is slightly larger than the diameter of the input bar. That clearance between the input bar and the output bar acts as the additional parts of the previous configuration.

The main difference between this specimen and a double-notched specimen is the width of the shear area, called the shear band. By using the punch specimen, the shear band becomes larger than the clearance between the pressure bars, making it impossible to know the exact value of the shear band. A double-notched specimen lets us define the shear band only by changing the dimensions. In order to control the shear band, a new technique was developed by modifying the punch test. A punch specimen with notch is used (Figure 2(e)) instead of the former one (Figure 2(d)).

This paper discusses five specimen geometries used in the SHSB test, i.e. (1) circular hat-shaped (C-HS), (2) flat hat-shaped (F-HS), (3) double-notch (D-N), (4) punch without notch (P-N), and (5) punch with notch (P-nN). These three techniques (hat-shaped, double-notch and punch) may generate different test results due to differences in pressure bar, specimen, shear geometry, etc. Therefore, the main purpose of this study was to compare these three SHSB techniques to determine the shear stress-shear strain of the specimen. An aluminum alloy (2024-T351) was used as the material of the specimen that was tested at a high strain rate. Aluminum was selected for its well-known properties of strain rate insensitivity. The study was mainly conducted by a numerical simulation. On the SHSB, the test should generate a pure shear state such that the shear stress-shear strain curve can be extracted from the recorded data.

2 Description of Split Hopkinson Shear Bar Technique

The apparatus of the split Hopkinson shear bar is similar to the split Hopkinson pressure bar. It consists of four main components: striker bar, input bar, specimen, and output bar. Figure 1 shows a schematic of the three techniques of using the SHSB apparatus. Each technique has the same length of striker bar, input bar, and output bar, but they are different in diameter. The dimensions are specified in Table 1.

Table 1 Dimension specifications of the bars.

SHSB Techniques	Outer Diameter (Do, mm)	Inside Diameter (Di, mm)	Length (L, mm)
Striker Bar (SB)			
Hat-Shaped	14.50	-	300
Punch	6.18	-	300
Double-Notch	11.50	-	300
Input Bar (IB)			
Hat-Shaped	14.50	-	1200
Punch	6.18	-	1200
Double-Notch	11.50	-	1200
Output Bar (OB)			
Hat-Shaped	14.50	-	1200
Punch	12.70	6.40	1200
Double-Notch	17.80	12.60	1200

2.1 Hat-shaped Test

The hat-shaped test can be categorized according to two geometries, i.e. a circular geometry (Figure 2(a)) and a flat geometry (Figure 2(b)). Both geometries have a specific shear area in which the adiabatic shearing is located

[9,10]. Meanwhile, the pressure bar is made of a solid cylindrical bar with the same diameter. The dimensions of the hat-shaped specimen that was used in this study are listed in Table 2 and the geometry is shown in Figure 2(a) for the circular hat-shaped specimen and in Figure 2(b) for the flat hat-shaped specimen.

Table 2 Dimensions of hat-shaped specimen.

Dimension	Symbol	Value (mm)	
		Circular Hat-shaped	Flat Hat-shaped
Outer diameter 1	*OD1*	14.000	13.000
Outer diameter 2	*OD2*	7.000	5.600
Inside diameter	*ID*	7.200	6.000
Depth of ID	*D*	8.000	8.000
Height of OD1	*H*	9.100	10.100
Total length of specimen	*L*	14.000	14.000
Width	*W1*	-	6.000
Bottom height	*H2*	-	5.000

2.2 Double-notch Test

In the SHSB test with the double-notch technique, the input bar is a solid cylinder and the output bar is a hollow cylinder/pipe. The specimen used in this technique is a flat plate that has two pairs of notches that will be cut off to create the geometry shown in Figure 2(c) and Table 3.

Table 3 Dimension of double-notched specimen.

Dimension	Symbol	Value (mm)
Length of specimen	*L*	17.000
Width of specimen	*W*	4.800
Depth of specimen	*D*	5.000
Inner length	*L1*	11.500
Height of shear zone	*h*	2.590
Clearance	*c*	0.230

2.3 Punch Test

Similar to the double-notch technique, this test uses a solid cylinder for the input bar and a hollow cylinder/pipe for the output bar. The inside diameter of the output bar is slightly larger than the outside diameter of the input bar to accommodate the shear deformation. In this paper, the author made two types of punch specimens, i.e. a punch specimen without notch (Figure 2(d)) and a punch specimen with notch (Figure 2(e)). The punch specimen with notch was made to generate a stress concentration in a specific shear area. With this notch, the

shear area is easier to define. The dimensions and geometry of the punch test specimens are shown in Tabel 4 and Figure 2(d) (without notch) and 2(e) (with notch).

Table 4 Dimension of punch specimen.

Dimension	Symbol	Value (mm)
Outer diameter	*OD1*	12.700
Inside diameter	*ID*	6.180
Height of shear zone	*h*	1.260
Clearance	*c*	0.110
Thickness of specimen	*T*	5.000

3 Data Analysis and Calculation

Gray II [16] presents the theory of one-dimensional stress wave propagation in the Hopkinson bar.

This theory can be applied with assumptions such as: homogeneous and isotropic bars; a uniform cross-sectional area and a straight neutral axis; the bar being elastic during the test with no dispersion; the specimen undergoing uniform deformation; a force equilibrium on the surface of the specimen in contact with the input and output bars [17].

The strain waves ($\varepsilon_i, \varepsilon_r, and\ \varepsilon_t$) were used to determine the equation of shear stress (τ), shear strain (γ), and shear strain rate ($\dot{\gamma}$) of the specimen, which can be expressed in 1-wave analysis as follows [17]:

$$\tau(t) = \frac{EA_t\varepsilon_t \cos\theta}{A_s} \tag{1}$$

$$\gamma(t) = \frac{c_0}{L_s}\left(\left(1+\frac{A_i}{A_t}\right)\int_0^t \varepsilon_r\, dt - \left(1-\frac{A_i}{A_t}\right)\int_0^t \varepsilon_i\, dt\right) \tag{2}$$

$$\dot{\gamma}(t) = \frac{c_0}{L_s}\left(\left(1+\frac{A_i}{A_t}\right)\varepsilon_r(t) - \left(1-\frac{A_i}{A_t}\right)\varepsilon_i(t)\right) \tag{3}$$

where, E is Young's modulus of the bar, A_i, A_t and A_s are the cross-section areas of the input bar, the output bar and the specimen, respectively; ε_i and ε_t is the incident and the transmitted strain wave, respectively; θ is the shear angle, c_0 is the longitudinal wave velocity in the bar = 5386 m/s, L_s is the length of the shear area.

The shear stress (τ), shear strain (γ), and shear strain rate ($\dot{\gamma}$) for each specimen can be calculated using Eqs. (1) to (3), respectively:

Circular Hat-shaped specimen (Figure 2(a))

$$A_i = A_t = cross - section\ of\ input\ /\ output\ bar = \frac{\pi}{4}\phi IB^2 = \frac{\pi}{4}\phi OB^2 \quad (4)$$

$$A_s = \pi\left(\frac{ID+OD2}{2}\right)\sqrt{\left(\frac{ID-OD2}{2}\right)^2 + (H-D)^2} \quad (5)$$

$$L_S = \frac{ID-OD2}{2} \quad (6)$$

$$\theta = \tan^{-1}\left(\frac{\frac{ID-OD2}{2}}{H-D}\right) \quad (7)$$

Flat Hat-shaped specimen (Figure 2(b))

$$A_i = A_t = cross - section\ of\ input\ /\ output\ bar = \frac{\pi}{4}\phi IB^2 = \frac{\pi}{4}\phi OB^2 \quad (8)$$

$$A_s = \pi W_1\sqrt{\left(\frac{ID-OD2}{2}\right)^2 + (H-D)^2} \quad (9)$$

$$L_S = \frac{ID-OD2}{2} \quad (10)$$

$$\theta = \tan^{-1}\left(\frac{\frac{ID-OD2}{2}}{H-D}\right) \quad (11)$$

Double-notch specimen (Figure 2(c))

$$A_i = cross - section\ of\ input\ bar = \frac{\pi}{4}\phi IB^2 \quad (12)$$

$$A_t = cross - section\ of\ hollow\ output\ bar = \frac{\pi}{4}\left(\phi {OB_1}^2 - \phi {OB_2}^2\right) \quad (13)$$

$$A_s = 2W\sqrt{c^2 + h^2} \quad (14)$$

$$L_s = c$$

$$\theta = \tan^{-1}\left(\frac{c}{h}\right) \quad (15)$$

Punch specimen (Figure 2(d) & Figure 2(e))

$$A_i = cross - section\ of\ input\ bar = \frac{\pi}{4}\phi IB^2 \quad (16)$$

$$A_t = cross - section\ of\ hollow\ output\ bar = \frac{\pi}{4}\left(\phi {OB_1}^2 - \phi {OB_2}^2\right) \quad (17)$$

$$A_s = \pi(w + ID)\sqrt{c^2 + h^2} \quad (18)$$

$$L_s = c \quad (19)$$

$$\theta = \tan^{-1}\left(\frac{c}{h}\right) \quad (20)$$

4 Numerical Simulation and Validation

Five numerical simulations were conducted to simulate the three SHSB techniques using ABAQUS/CAE®, i.e. (1) circular hat-shaped specimen (C-HS), (2) flat hat-shaped specimen (F-HS), (3) double-notch specimen (D-N), (4) punch specimen without notch (P-nN), and (5) punch specimen with notch (P-N).

4.1 Finite Element Modeling and Parameters

The modeling was conducted in a half or a quarter 3D solid model in order to minimize the simulation time for the same result, for making a comparison to a complete solid 3D model. Maraging steel material (AISI Grade 16Ni) was applied for all bar components [17], and aluminum alloy 2024-T351 was applied for all specimens, where the Johnson-Cook constitutive material model was used [18].

Table 5 describes the mechanical properties of aluminum alloy 2024-T351, while Table 6 describes the Johnson-Cook parameter for this material.

The same kinetic energy $\left(EK = \frac{1}{2}mV^2\right)$, where, $\boldsymbol{m}$ and $\boldsymbol{V}$ are the mass and the velocity of the striker bar, was applied to facilitate the same input parameters for each technique. Since the mass of the striker bar was different for each technique, the striker bar velocity had to be varied such that the input energy was the same for each technique. For kinetic energy at about 7.337 Joule, the initial striker bar velocities that should be given were 6.058 m/s (for the hat-shaped test), 14.215 m/s (for the punch test), and 7.639 m/s (for the double-notch test). The gap between the striker bar and the input bar was set to 0.1 mm in order to minimize the total time of analysis.

The meshing of the bars was selected with an element size of approximately 2×2×2 mm. Meanwhile, a smaller element size of approximately 1×1×1 mm was selected for the specimen. Hexagonal (C3D8R) element type was assigned for both the bars and the specimen.

Table 5 Mechanical properties of AA 2024-T351 [18].

Material Properties	Symbol	Value	Unit
Density	P	2770	kg/m^3
Young's modulus	E	73.084	GPa
Shear modulus [1]	G	27.481	GPa
Poisson ratio	υ	0.33	-

[1] Recalculated from E = 2×G×(1+ *ν)*

Table 6 Johnson-Cook parameter for AA 2024-T351 [18].

Material Properties	Symbol	Value	Unit
(a) Strength parameters			
Static yield limit	A	265	MPa
Strain hardening modulus	B	426	MPa
Strain hardening exponent	n	0.34	-
Strain rate coefficient	C	0.015	-
Thermal softening exponent	m	1.0	-
Melting temperature	T_{melt}	775	°K
Transition temperature	T_{trans}	294	°K
(b) Damage Parameters			
D_1		0.13	-
D_2		0.13	-
D_3		-1.5	-
D_4		0.011	-
D_5		0	-
(c) Mie-Grunesien EOS Parameters			
S_1		1.338	-
S_2		0	
S_3		0	
γ_0		2	-

A convergency test was conducted to study the effect of mesh size on the generated results. The elements in the shear zone area were varied at 50 μm, 30 μm, 20 μm, 15 μm, and 10 μm. The study was conducted using a circular hat-shaped geometry (see Figure 3).

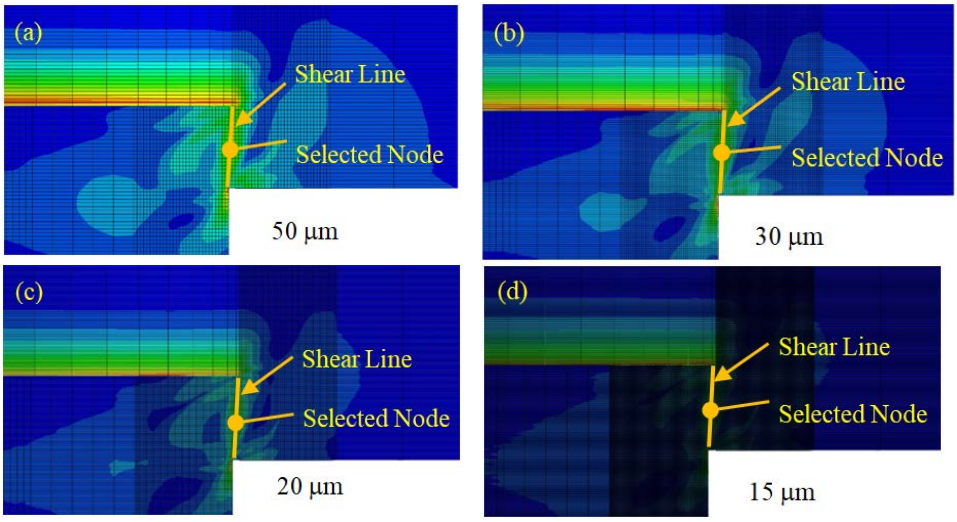

Figure 3 Mesh size of (a) 50 μm, (b) 30 μm, (c) 20 μm, (d) 15 μm.

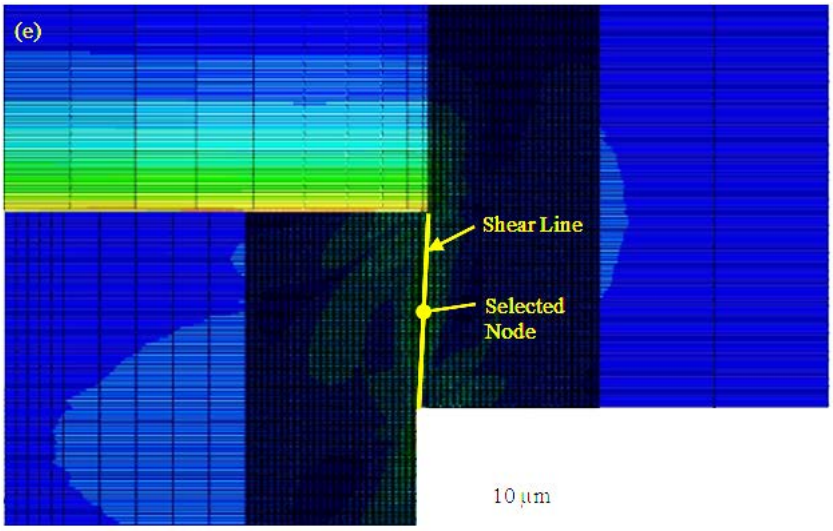

Figure 3 ***Continued*****.** Mesh size of (e) 10 µm.

A comparison of shear, radial and axial stresses at the selected node (see Figure 3) in the mid-length of the shear line for various mesh sizes is shown in Figure 4. It shows that the shear stress for all mesh sizes was the same, while its values varied for radial and axial stresses. Thus, an element size of 20 µm was used for the shear area to generate the convergence results.

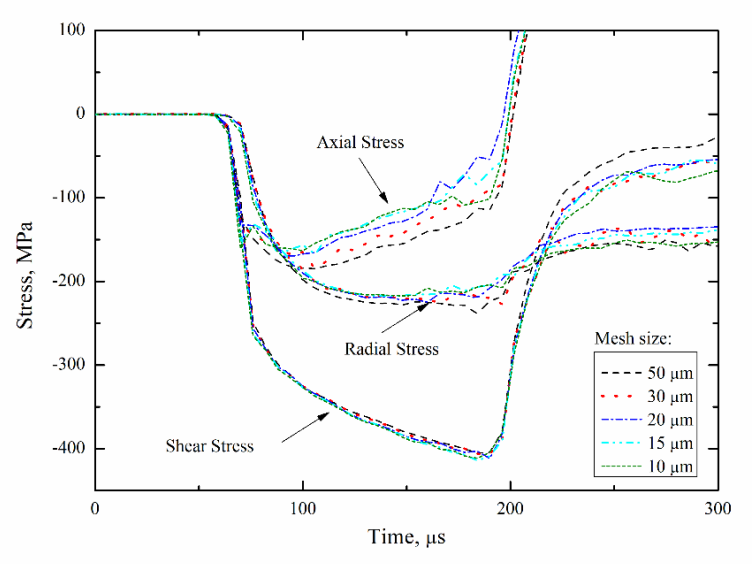

Figure 4 Comparison of shear, radial, and axial stresses for varied mesh sizes.

4.2 Validation of the Finite Element Model

Validation of the finite element model was conducted to determine the right selection of the parameters, the boundary conditions and the loading conditions in the numerical simulation. The validation was conducted by comparing the value of the numerical simulation with: (i) a theoretical value and (ii) experimental data.

The first step of validation was conducted to check whether the finite element model can simulate the elastic wave propagation in the bar or not. It was conducted by comparing the amplitude of the incident wave from the theoretical value with the value from the numerical simulation. The validation utilized the theory of one-dimensional waves ranging from momentum to momentum due to the impact of the striker bar. The amplitude of the strain wave, ε, propagated in the input bar due to a solid bar impact was then calculated as:

$$\varepsilon = \frac{V}{2c_0} \tag{21}$$

Figure 5(a) shows the incident wave generated from the element in the numerical simulation. The simulation was conducted using a bar diameter of 14.5 mm with the striker bar velocity at 10.915 m/s (the same value as in the experimental data). Based on the simulation, the average value for the incident wave was 1015 με. The theoretical value of the incident wave was then calculated using Eq. 21 with V = 10.915 m/s and c_0 = 5386 m/s, which yielded 1013 με. The difference between the numerical simulation and the theoretical value was less than 1%. Furthermore, the elastic wave propagation was also represented well in the strain wave (sinusoidal fluctuation).

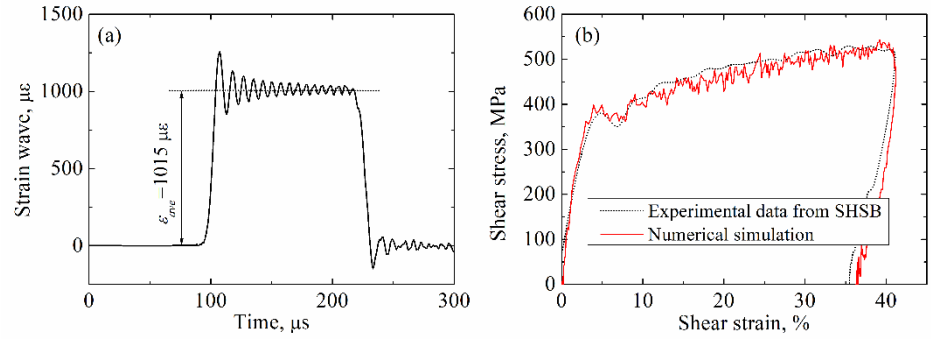

Figure 5 Validation using: (a) theoretical value, (b) experimental data.

The second validation was conducted to check whether the model could represent the plastic deformation in the specimen or not. It was conducted by

comparing the numerical simulation result with the experimental result. The experiment was conducted at Swinburne University of Technology, Australia. A pressure bar diameter of 14.5 mm was used. The bar was made of maraging steel. The specimen used in the experiment was hat-shaped. The striker bar velocity was 10.915 m/s. More details with regard to the experimental setup can be found in References [17] and [19].

Meanwhile, the numerical simulation parameters were set the same as the experimental ones, i.e. the same number of components and their dimensions, the same mechanical properties of the bar and specimen, the same striker bar velocity, etc. The strain signals (ε_i, ε_r and ε_t) were generated from a selected element where the strain gauge was located in the experiment. These signals were then processed using Eqs. 1-7 to generate the stress-strain curve. A comparison of the stress-strain curves from the numerical simulation and the experimental result are shown in Figure 5(b). The average flow stress in the experiment was 495.2 MPa, while in the numerical simulation it was 478.3 MPa. The difference was 3.4%. This validation shows that the developed model could represent the plastic deformation in the specimen quite well.

Both validations gave a difference of less than 4%. The elastic wave propagation in the bar and the plastic deformation of the specimen could be reproduced well by the model. Therefore, it can be concluded that the correct parameters had been assigned in the modeling and that the model can be used for other parametric studies of the SHSB.

5 Results and Discussion

The finite element models were developed for three SHSB techniques, i.e. hat-shaped, double-notched, and punch tests. Five specimen geometries, i.e. circular hat-shaped (C-HS), flat hat-shaped (F-HS), double-notch (D-N), punch without notch (P-nN), and punch with notch (P-N), were studied. For comparable results, the specimens should have the same shear area (± 25 mm^2) and shear angle (± 5 deg) as described in Table 7. The geometry of the specimens was set such that it may compensate ±1 mm in the manufacturing process.

Table 7 Shear area and angle for four types of specimens.

Specimen Geometry	Shear Area, mm^2	Shear Angle, deg
Circular Hat-Shaped (C-HS)	24.64	5.19
Flat Hat-Shaped (F-HS)	25.31	5.44
Double-Notch (D-N)	24.99	4.99
Punch w/o notch (P-nN)	24.99	4.99
Punch w/ notch (P-N)	24.96	5.07

Data analysis and processing were conducted similar to those in the experiment. The incident, reflected and transmitted waves ($\varepsilon_i, \varepsilon_r$ and ε_t) were taken from the element where the strain gauges were located. Those three waves then should be placed in the same time windows using Lifshitz and Leber's method [20] (see Figure 6(a) for an example of the three waves taken from C-HS testing). The shear stress-time, shear strain-time and shear strain rate-time relation were calculated using the formulas given in Eqs. (1) to (20).

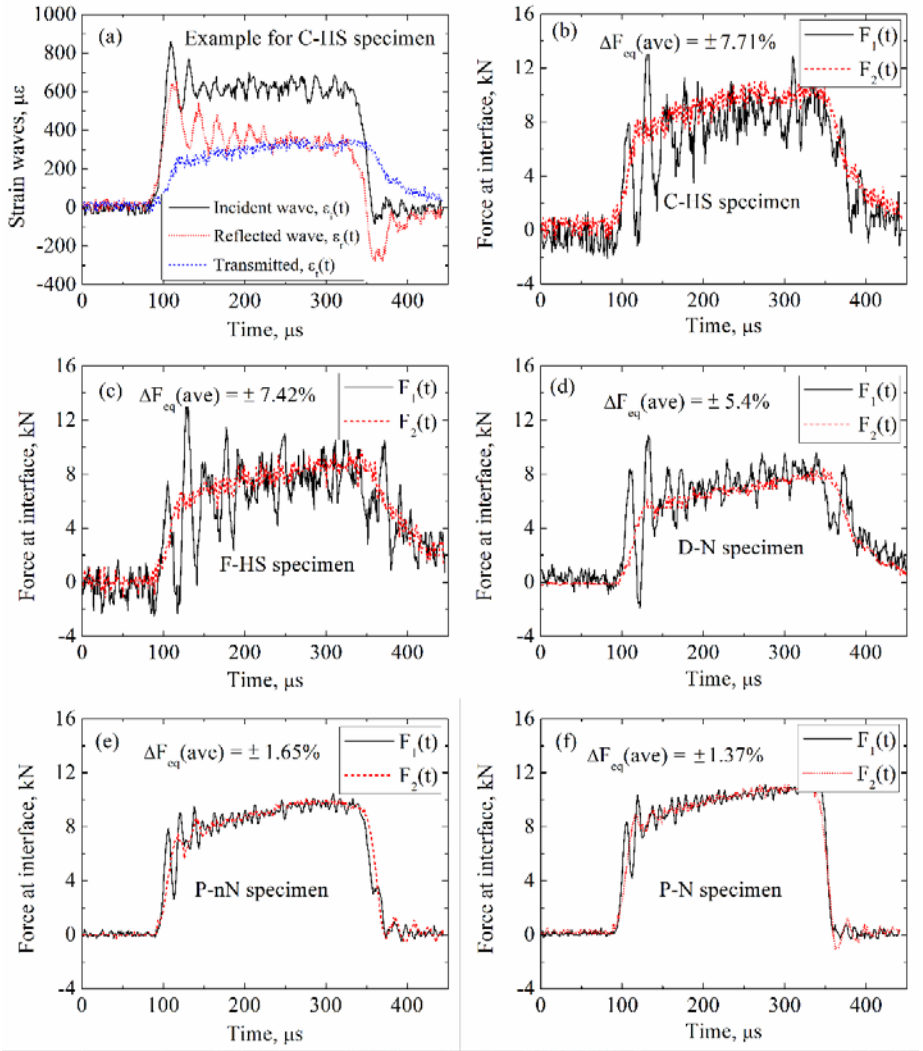

Figure 6 (a) Example of incident, reflected and transmitted waves from C-HS testing. Force equilibrium conditions for: (b) C-HS, (c) F-HS, (d) D-N, (e) P-nN and (f) P-N testing.

The force equilibrium was checked to ensure that the equilibrium assumption was fulfilled (see Figures 6(b) to 6(f)). The average percentage of discrepancy between F_1 and F_2 was calculated as [21]:

$$\Delta F_{eq}(ave) = \pm \frac{\sum_i^n \frac{F_{1i}-F_{2i}}{F_{2i}}}{2n} \times 100\% \quad (22)$$

The force equilibrium for each test is tabulated in Table 8. These results show that the punch test generated a less fluctuating force equilibrium ($\Delta F_{eq}(ave)$ in the range of ±1.37% to ±1.67%) compared to the other techniques. This means that during the test, the punch specimen received an equivalent magnitude of force between the force at the input bar-specimen interface and the specimen-output bar interface. Thus, the validity of the test was confirmed. For the other techniques, the force equilibrium was achieved after 3-4 reverberations like in the regular SHPB test. The maximum force equilibrium discrepancy was ±7.71%, which is acceptable [22]. Thus, the generated data can be used to generate further shear stress-shear strain curves.

Table 8 Numerical simulation results comparison.

SHSB Tech.	$\Delta F_{eq}(ave)$ (%)	Shear Strain Rate Grad. (s^{-2})	Average Shear Strain Rate (s^{-1})	Final Shear Strain (%)	Average Shear Flow Stress (MPa)
C-HS	7.71	-33.3	33,087	4.48	336.5
F-HS	7.42	-18.2	17,963	2.42	313.2
D-N	5.40	-24.5	18,544	2.44	275.9
P-nN	1.65	-96.7	35,613	5.08	308.6
P-N	1.37	-93.6	24,378	3.61	365.6

Table 8 shows a comparison of shear strain rate gradient, average shear strain rate, final shear strain and average shear stress for a strain range from 1 to 2 mm/mm. A smaller value of the strain rate gradient (see Figure 7) means that the specimen received a more constant strain rate during the test, which is desired. Thus, the F-HS specimen is the best option.

In terms of strain rates, the P-N and C-HS specimens generated the highest magnitude among the techniques, i.e. approximately 35,000 s^{-1}. Since aluminum is known for its strain rate insensitivity, the flow stress should not be influenced by the magnitude of the strain rate during the test. Thus, we can ignore the strain rate effects.

Figure 8 shows the shear stress-shear strain curves generated from the numerical simulations. It can be seen than even though the five specimens were maintained at a similar shear area (±25 mm^2) and a shear angle (±5°), they generated different flow shear stresses (in a range of 275 to 365 MPa). The D-N specimen generated the lowest flow stress (275 MPa).

In this first study, the shear angle was set to ±5° so that the shear stress to be measured was dominant, even though there is evidence that the radial and axial stresses still exist (see Figure 4). Based on the results of this study, the flow stresses are very sensitive to the geometry of the specimen.

The closest results in the material characterization using SHSB were produced by the hat-shaped (C-HS and F-HS) and the P-N technique. The hat-shaped technique should be selected if a stable strain rate is desired and the punch with notch technique should be selected if a more accurate force equilibrium is required.

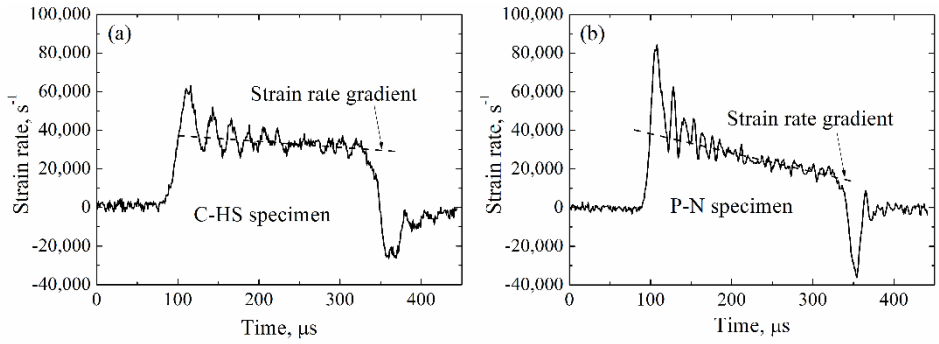

Figure 7 Example of shear strain rate curve for: (a) C-HS and (b) P-N.

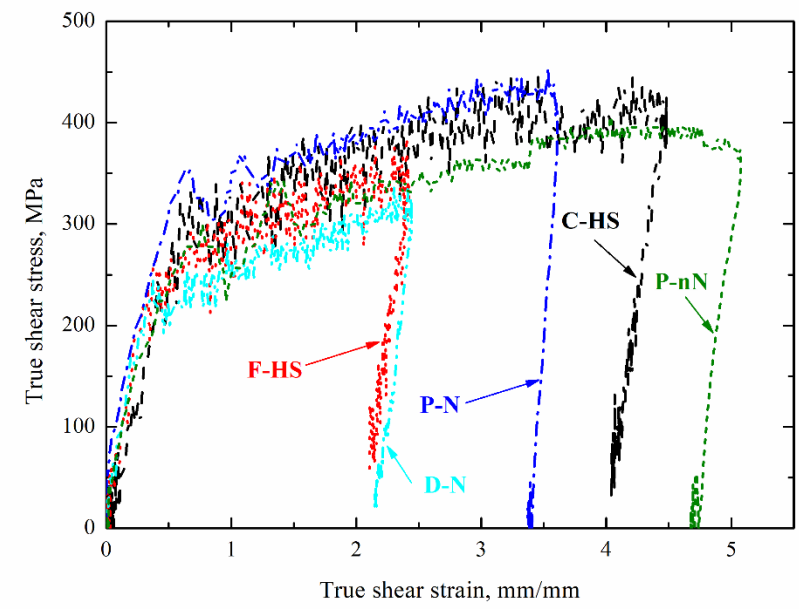

Figure 8 Shear stress-shear strain curve for three SHSB techniques.

In terms of ease of conducting the experiment, the order from the easiest to the hardest one is: hat-shaped (circular or flat), double notch, punch with notch, and punch without notch. The double-notch and punch techniques use a hollow output bar, where the availability and machinability of the bars are limited. Moreover, the inner diameter of the output bar should be changed for different shear angles, meaning that the test should use a different output bar. The hardest test is when conducting the punch without notch specimen. The exact value of the shear band cannot be determined, and the shear angle can only be predicted from the gap between the outside diameter of the input bar and the inside diameter of the output bar. Meanwhile, for the hat-shaped (circular or flat) technique, a regular SHPB testing (solid input and output bars) can be used. Different shear angles can be directly tested without changing the setting of the pressure bar. The apparatus can also be used for a compression test as in classic the SHPB test. A solid bar with a ratio of $L/D \geq 100$ is also easier to machine, compared to a hollow one.

In terms of the machinability of the specimen, the order from the easiest to the hardest is: punch without notch, circular hat-shaped, flat hat-shaped, double-notch, and punch with notch. The last two geometries are quite hard to manufacture for small shear angles.

This initial study showed that each technique has its own advantages and disadvantages and that they generate different shear stress-shear strain curves, which is not desirable. This study was conducted only for a shear angle of ±5°; therefore, more deep analysis will be conducted in the future for different sets of shear area and shear angle in order to study the effect of specimen geometries and techniques in the SHSB test results.

6 Conclusions

Numerical simulations were successfully conducted to simulate three split Hopkinson shear bar techniques, i.e. hat-shaped, double-notch, and punch. The validation showed that the developed models were able to reproduce both the elastic wave propagation in the bar and the plastic deformation of the specimen; thus, they can be used for further comparison studies of SHSB techniques. The validity of the test was checked by comparing the force equilibrium condition for each test, where all tests satisfied the assumption of a valid SHPB test. The maximum force equilibrium discrepancy was ±7.71%, which is acceptable.

This study successfully tested and compared three SHSB techniques with a number of considerations, i.e. the same parameter values for kinetic energy (7.337 Joule), shear area (±25 m^2) and shear angle (±5°). From the numerical

simulation results, the average shear flow stress was in the range of 275.9 to 365.6 MPa. The final shear strain was in the range of 2.42 to 5.08 mm/mm. The average strain rate was in the range of 17,963 to 35,613 s^{-1}. The force equilibrium discrepancy was in the range of ±1.37 to ±7.71 %, and the shear strain rate gradient was in the range of 18.2 to 96.7 s^{-2}.

The results show that different techniques generate different shear stress-shear strain curves, which is not desirable. Based on the smallest force error and strain rate gradient, the hat-shaped technique can be chosen if a stable strain rate is desired, while the punch with notch technique can be selected if a more accurate force equilibrium is required. However, other factors such as the machinability of the bar and specimen, and the ease of conducting the experiment also need to be considered. As the optimum option considering all factors, the authors recommend the hat-shaped technique (either circular or flat) for experimentally studying the effect of shear angle on an SHSB specimen.

Acknowledgement

This work was carried out at the Engineering Design Laboratory Mechanical Engineering Department, Faculty of Mechanical and Aerospace Engineering, Institut Teknologi Bandung and was financially supported by Institut Teknologi Bandung through P3MI (*Program Penelitian Pengabdian Masyarakat dan Inovasi*).

References

[1] Nemat-Nasser, S., *Introduction to High Strain Rate Testing*, in Kuhn, H & Medlin, D, A*SM Handbook: Mechanical Testing and Evaluation*, **8**, ASM International, pp. 427-428, 2000.

[2] Hopkinson, J., *On the Rupture of Iron Wire by a Blow*, in Proceedings of the Manchester Literary and Philosophical Society, pp. 40-45, 1872.

[3] Hopkinson, J., *Further Experiments on the Rupture of Iron Wire*, in Proceedings of the Manchester Literary and Philosophical Society, pp. 119-121, 1872.

[4] Hopkinson, B., *A Method of Measuring the Pressure Produced in the Detonation of High, Explosives or by the Impact of Bullets*, Philosophical Transactions of the Royal Society of London. Series A, Containing Papers of a Mathematical or Physical Character, **213**(497-508), pp. 437-456, 1914.

[5] Davies, R.M. & Taylor G.I., *A Critical Study of the Hopkinson Pressure Bar*, Philosophical Transactions of the Royal Society of London, Series A, Mathematical and Physical Sciences, **240**(821), pp. 375-457, 1948.

[6] Kolsky, H., *An Investigation of the Mechanical Properties of Materials at Very High Rates of Loading*, Proceedings of the Physical Society. Section B, **62**(11), pp. 676-700, 1949.
[7] Hartmann, K-H., Kunze, H-D. & Meyer, L.W., *Metallurgical Effects on Impact Loaded Materials, Shock Waves and High-Strain-Rate Phenomena* in Meyers, M.A. & Murr, L.E., *Metals: Concepts and Applications*, Springer US, pp. 325-337, 1981.
[8] Beatty, J.H., Meyer, L.W., Meyers, M.A. & Nemat-Nasser, S., *Formation of Controlled Adiabatic Shear Bands in AISI 4340 High Strength Steel*, in Meyers, M.A., Murr, L.E. & Staudhammer, K.P., *Shock Wave and High-Strain-Rate Phenomena in Materials*, Marcel Dekker, New York, United States, pp.645-656, 1992.
[9] Piers, J., Verleysen, P. & Degrieck, J., *The Use of Hat-Shaped Specimens for Dynamic Shear Testing*, Foundations of Civil and Environmental Engineering, **11**, pp. 97-111, 2008.
[10] Peirs, J., Verleysen, P., Degrieck, J. & Coghe, F., *The Use of Hat-Shaped Specimens to Study the High Strain Rate Shear Behaviour of Ti–6Al–4V*, International Journal of Impact Engineering, **37**(6), pp. 703-714, 2010
[11] Dowling, A.R. *The Dynamic Punching of Metals*, Journal of Institute of Metals, **98**, pp. 215-224, 1970.
[12] Ferguson, W.G., Hauser, F.E. & Dorn, J.E., *Dislocation Damping in Zinc Single Crystals*, British Journal of Applied Physics, **18**(4), pp. 411-417, 1967.
[13] Campbell, J.D. & Ferguson, W.G., *The Temperature and Strain-Rate Dependence of the Shear Strength of Mild Steel*, The Philosophical Magazine: A Journal of Theoretical Experimental and Applied Physics, **21**(169), pp. 63-82, 1970.
[14] Harding, J. & Huddart, J., *The Use of the Double-Notch Shear Test in Determining the Mechanical Properties of Uranium at Very High Rates of Strain*, Institute of Physics, 1980.
[15] Harding, J., *High-Rate Straining and Mechanical Properties of Materials*, *Explosive Welding*, Forming and Compaction, Blazynski T.Z., Springer Netherlands, pp. 123-158, 1983.
[16] Gray, G.T., III, *Classic Split Hopkinson Pressure Bar Testing* in Kuhn, H. & Medlin, D., *ASM Handbook: Mechanical Testing and Evaluation*, **8**, ASM International, pp. 462-476, 2000.
[17] Kariem, M.A., *Reliable Materials Performance Data from Impact Testing*, Doctor of Philosophy, Faculty of Engineering and Industrial Sciences, Swinburne University of Technology, Hawthorn, 2012.
[18] Johnson, G.R. & Cook, W.H., *A Constitutive Model and Data for Metals Subjected to Large Strains, High Strain Rates, and High Temperatures*, in Proceeding of the 7th International Symposium in Ballistics, pp. 541-547, 1983.

[19] Edwards, N.J., Kariem, M.A., Rashid, R.A.R., Cimpoeru S.J., Lu G. & Ruan D., *Dynamic Shear Testing of 2024 T351 Aluminium at Elevated Temperature*, Materials Science and Engineering: A, **754**, pp. 99-111, 2019.

[20] Lifshitz, J.M. & Leber, H., *Data Processing in the Split Hopkinson Pressure Bar Tests*, International Journal of Impact Engineering, **15**(6), pp. 723-733, 1994.

[21] Kariem, M., Ruan, D., Beynon, J. & Prabowo, D., *Mini Round-Robin Test on the Split Hopkinson Pressure Bar*, Journal of Testing and Evaluation, **46**(2), pp. 457-468, 2018.

[22] Kariem, M.A., Santiago R.C., Govender R., Shu D.W., Ruan D., Nurick G., Alves, M., Lu, G. & Langdon, G.S., *Round-Robin Test of Split Hopkinson Pressure Bar*, International Journal of Impact Engineering, **126**, pp. 62-75, 2019.